

# Current Biology

## Behavioral Responses to a Repetitive Visual Threat Stimulus Express a Persistent State of Defensive Arousal in *Drosophila*

### Highlights

- A novel behavioral assay using repeated, visual threat stimuli is characterized
- Flies show persistent defensive responses including running, jumping, and freezing
- Velocity and hopping frequency scale with stimulus number and with stimulus frequency
- *Drosophila* genetics can now be used to investigate a persistent defensive state

### Authors

William T. Gibson,  
Carlos R. Gonzalez, ..., Pietro Perona,  
David J. Anderson

### Correspondence

wtgibson@caltech.edu (W.T.G.),  
wuwei@caltech.edu (D.J.A.)

### In Brief

Using a novel, repetitive, visual threat stimulus paradigm (termed ReVSA), Gibson et al. investigate a defensive state in *Drosophila*, perhaps analogous to fear. ReVSA behaviors include running, jumping, and freezing. Defensive states can now be probed in a genetically tractable insect species.



# Behavioral Responses to a Repetitive Visual Threat Stimulus Express a Persistent State of Defensive Arousal in *Drosophila*

William T. Gibson,<sup>1,2,3,\*</sup> Carlos R. Gonzalez,<sup>3</sup> Conchi Fernandez,<sup>3</sup> Lakshminarayanan Ramasamy,<sup>4</sup> Tanya Tabachnik,<sup>4</sup> Rebecca R. Du,<sup>2</sup> Panna D. Felsen,<sup>3</sup> Michael R. Maire,<sup>3</sup> Pietro Perona,<sup>3</sup> and David J. Anderson<sup>1,2,4,\*</sup>

<sup>1</sup>Howard Hughes Medical Institute, California Institute of Technology, Pasadena, CA 91125, USA

<sup>2</sup>Division of Biology & Biological Engineering 156-29, California Institute of Technology, Pasadena, CA 91125, USA

<sup>3</sup>Division of Engineering & Applied Sciences 136-93, California Institute of Technology, Pasadena, CA 91125, USA

<sup>4</sup>Janelia Farm Research Campus, Howard Hughes Medical Institute, 19700 Helix Drive, Ashburn, VA 20147, USA

\*Correspondence: [wtgibson@caltech.edu](mailto:wtgibson@caltech.edu) (W.T.G.), [wuwei@caltech.edu](mailto:wuwei@caltech.edu) (D.J.A.)

<http://dx.doi.org/10.1016/j.cub.2015.03.058>

## SUMMARY

The neural circuit mechanisms underlying emotion states remain poorly understood. *Drosophila* offers powerful genetic approaches for dissecting neural circuit function, but whether flies exhibit emotion-like behaviors has not been clear. We recently proposed that model organisms may express internal states displaying “emotion primitives,” which are general characteristics common to different emotions, rather than specific anthropomorphic emotions such as “fear” or “anxiety.” These emotion primitives include scalability, persistence, valence, and generalization to multiple contexts. Here, we have applied this approach to determine whether flies’ defensive responses to moving overhead translational stimuli (“shadows”) are purely reflexive or may express underlying emotion states. We describe a new behavioral assay in which flies confined in an enclosed arena are repeatedly exposed to an overhead translational stimulus. Repetitive stimuli promoted graded (scalable) and persistent increases in locomotor velocity and hopping, and occasional freezing. The stimulus also dispersed feeding flies from a food resource, suggesting both negative valence and context generalization. Strikingly, there was a significant delay before the flies returned to the food following stimulus-induced dispersal, suggestive of a slowly decaying internal defensive state. The length of this delay was increased when more stimuli were delivered for initial dispersal. These responses can be mathematically modeled by assuming an internal state that behaves as a leaky integrator of stimulus exposure. Our results suggest that flies’ responses to repetitive visual threat stimuli express an internal state exhibiting canonical emotion primitives, possibly analogous to fear in mammals. The mechanistic basis of this state can now be investigated in a genetically tractable insect species.

## INTRODUCTION

Emotions are internal states that are expressed by specific behaviors and that modulate perception, cognition, and communication [1–5]. Dysregulation of emotion systems is central to psychiatric disorders. Yet we still do not understand the general neural mechanisms that encode emotion states. Indeed, there is not even agreement on the causal relationship between emotion states and behavior, despite more than a century of debate beginning with Darwin [4] and William James [6, 7] (reviewed in [3, 8]). An understanding of emotion is therefore essential to explaining brain function, behavior, and evolution.

A mechanistic understanding of emotion states at the molecular and neural circuit levels would be aided by studying them in genetically tractable model organisms, especially invertebrates including insects such as *Drosophila* [3, 9–12]. Emotion research in animal models has traditionally been performed in mammalian systems, however [8, 13, 14], because they exhibit behavioral, physiological, and neuroanatomical homologies to humans [15]. Because of this bias, previous efforts to investigate “emotions” in insects (or other arthropod species) have involved attempts to identify behaviors or behavioral states exhibiting similarities to human emotions [10, 11, 16]. For example, traumatized bees have been shown to exhibit “pessimistic cognitive bias” in decision-making [17], and crayfish subjected to electric shocks have been suggested to exhibit “anxiety” [18].

Yet, distantly related species may express emotion states through behaviors that have no obvious homology to human behaviors. An alternative approach to identifying instances of emotional expression, which does not depend on anthropocentric homologies, is to establish general features of emotion states, or “emotion primitives,” which apply both to different emotions in a species and to emotions across phylogeny [3, 12, 19]. One can then search for behaviors that exhibit evidence of such emotion primitives in model organisms. We have recently suggested that such emotion primitives may include the following features or dimensions: persistence following stimulus cessation, scalability (a graded nature of the response), valence, generalization to different contexts, and stimulus degeneracy (different stimuli can evoke the same behavior by induction of a common emotion state) [3]. Although these primitives are

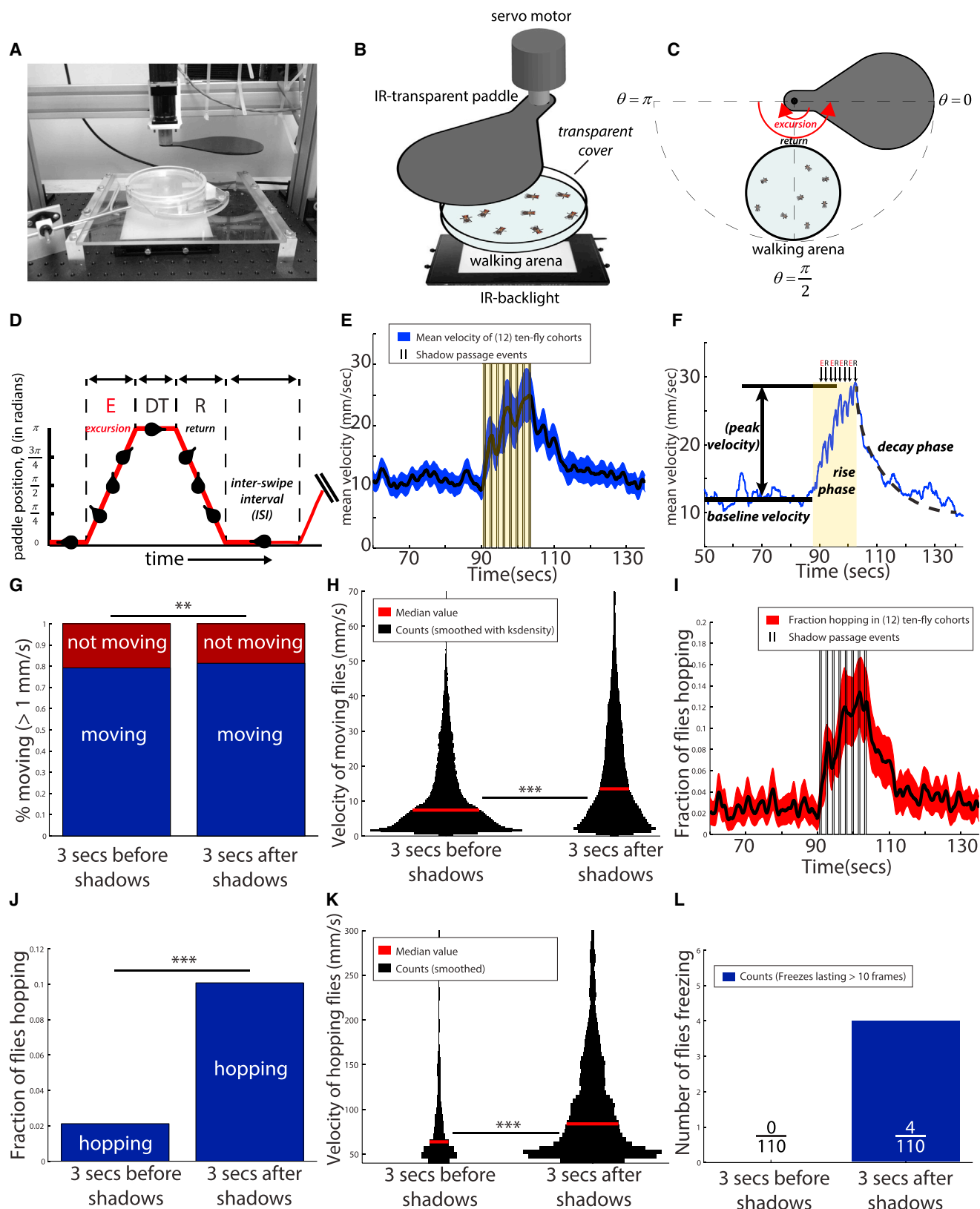


**Figure 1. Introduction to ReVSA**

(A and B) Shadow paddle apparatus.

(C) Motion of the shadow paddle.

(legend continued on next page)

features of internal emotion states, they should be reflected in the properties of behaviors that express such states.

Evidence of some of these properties in *Drosophila* has been provided using different behavioral paradigms. For example, flies are capable of entering states of persistent arousal, as evidenced by sustained locomotor activity [20–24] and/or neural activity [25, 26]. In some cases, these states exhibit “scalability”: the strength of the behavioral response scales in proportion to the number of stimuli or intensity of the stimulus [20]. *Drosophila* can be conditioned using either appetitive or aversive stimuli [27–32] (and both ethanol and sexual experience appear to be rewarding to them [33, 34]), demonstrating that these animals can represent valence internally. Flies that have been rejected by mating partners consume more ethanol, suggesting that rejection induces a state that generalizes to promote ethanol reward seeking [33]. In addition, flies have been shown to exhibit a “learned helplessness” response to an uncontrollable stressor [35], similar to rodents [36]. However, to our knowledge, there are few, if any, cases where evidence for multiple emotion primitives has been systematically investigated in a single behavioral paradigm.

Here, we establish and characterize a novel behavioral assay, termed ReVSA (repetitive visual stimulus-induced arousal), in which flies in an enclosed, inescapable arena are exposed to multiple passes of an overhead, translationally moving visual stimulus (rather than to a more traditional single-trial looming stimulus [37–39]). A simpler, manual version of this assay was previously explored by Kaplan and Trout [40]. This configuration affords systematic variation of stimulus parameters and quantitative analysis of the behavioral response, using automated tracking and behavior classifiers [41, 42]. Our results indicate that, under appropriate conditions, ReVSA responses exhibit evidence of persistence, scalability, valence, and generalizability. Importantly, flies show a cumulative response to successive stimulus presentations, provided that the inter-stimulus interval is sufficiently short. This property can be modeled by an internal state that behaves as a “leaky” integrator. These data suggest that escape responses to visual threat stimuli in *Drosophila* do not consist exclusively of single stimulus-response reflexes [37–39], but under certain conditions can exhibit integrative properties that reflect or express an underlying persistent defensive state. Together with recent studies of internal defensive states in mice [43, 44], our results provide evidence for a phylogenetic continuity of “emotion primitives,” and establish a behavioral assay for future mechanistic studies of the neural encoding of such states, in a genetically tractable invertebrate model organism.

## RESULTS

### *Drosophila* Exhibit Elevated Locomotor Activity in Response to a Moving Overhead Visual Stimulus

Our previous studies using the ReSH (repetitive startle-induced hyperactivity) assay suggested that *Drosophila* enter a state of persistent, elevated arousal when subjected to a staccato sequence of mechanical startle stimuli (air puffs) [20]. To develop a less traumatic and more ecologically relevant assay, we investigated whether a repeated sequence of overhead translational visual threat stimuli (hereafter referred to for simplicity as “shadows”) would elicit a similar persistent response. This question cannot be addressed in conventional looming stimulus response assays, which are single trial because the animal escapes [37–39, 45]. We therefore delivered sequences of shadows using a servo motor-driven, mechanically isolated infrared (IR)-transparent paddle controlled by custom software, which sweeps across a covered 100-mm walking arena from which the flies cannot escape (Figures 1A and 1B). Animals were video recorded at 33 Hz and tracked using custom-built machine vision software and behavior classifiers.

To characterize the flies’ responses to repetitive shadow stimuli, we first loaded cohorts of ten male flies into the walking arena and delivered eight consecutive shadow presentations at 1-s intervals (Figure 1E). For the first 90 s following introduction into the chamber, animals maintained a roughly constant baseline average velocity (Figures 1E and 1F; baseline velocity). Upon delivery of the train of shadow stimuli, animal movement increased markedly and continued to rise until termination of the stimulus (Figure 1F, rise phase), after which it gradually decayed back to baseline over a period of ~20 s (Figures 1E and 1F; decay phase). Importantly, the velocity of moving flies increased ( $p < .001$ ; Kruskal-Wallis test) to a greater extent than did the fraction of flies that were moving ( $p < .01$ ; chi-square test), 3 s after the shadow (Figures 1G and 1H). Therefore, locomotor velocity, not the percentage of moving flies, is the dominant component of the ReVSA response under these conditions.

To verify that the response to the paddle was indeed visual, we performed control experiments in which the paddle traversed a half-circle that did not overlap with the walking arena and hence was not visible to the flies as an overhead stimulus (Figures S1A–S1E). Under these conditions, no elevation in fly velocity (actually a decrease;  $p < .001$ ; Kruskal-Wallis test) was observed (red, Figures S1C and S1D). Furthermore, animals that happened to be standing upside down on the arena cover during shadowing did not respond to the paddle, suggesting that ReVSA is specific to overhead stimuli, consistent with shadow responses

(D) Control of swipe delivery. Dwell time (DT) and inter-shadow interval (ISI), respectively, control how long the paddle remains at  $\theta = \pi$  and  $\theta = 0$ .

(E) Canonical ReVSA curve for a cohort of ten male flies, with SEM envelopes. Shadow passes separated by an ISI of 1 s (vertical bars, black) cause an increase in velocity (yellow shaded region), which persists following stimulus cessation and then decays back to baseline.

(F) Illustration of baseline and peak height, as well as the three phases (“baseline,” “rise phase,” and “decay phase”).

(G) Proportion of flies moving in the 3 s before and after the shadow (\*\*, chi-square test).

(H) Velocities of moving flies, in the 3 s before and after the shadows (\*\*\*, Kruskal-Wallis test).

(I) Fraction of flies hopping over time (black), with SEM envelope (red).

(J) Fraction of flies hopping increases relative to baseline (\*\*\*, chi-square test).

(K) Velocity of hopping flies increases relative to baseline (\*\*\*, Kruskal-Wallis test). Sample size for panels (E)–(K) is  $n = 120$  flies.

(L) Number of flies freezing for  $\geq 10$  frames.

Asterisks represent  $p$  values, where (\*), (\*\*), and (\*\*\*) denote, respectively,  $p < .05$ ,  $p < .01$ , and  $p < .001$ . We use  $\alpha = 0.05$ .

previously studied in mice [46]. Finally, flies did not elevate their locomotor activity in response to flashing overhead lights (Movie S3), indicating that the ReVSA response requires translational paddle motion.

### The Response to the Shadow Paddle Includes Hopping as well as Walking

We next investigated whether the increase in velocity caused by the shadow was reflected only in walking, or whether other behaviors were also involved. Jumping responses to initiate flight have been previously observed in response to looming stimuli [37, 47]. We observed repeated and persistent jumping in response to repetitive shadow presentations, which we term “hopping” (Movie S1). We quantified hopping as movement above a particular threshold speed, selected based on a discontinuity in the population velocity distribution; this classifier was validated by manual scoring of videos (Experimental Procedures). Using this metric, we observed a rise in the fraction of hopping flies ( $p < .001$ ; chi-square test) during the shadow presentation (Figures 1I and 1J), which persisted for 20–30 s following shadow termination (Figure 1I). Furthermore, the average velocity of hopping flies increased relative to baseline ( $p < .001$ ; Kruskal-Wallis test) during the 3 s after the shadow (Figure 1K). Thus, fly cohorts responded to the shadow stimulus with both an increase in average locomotor velocity and an increase in hopping, indicating that they exhibit both quantitative increases and qualitative changes in their escape behavior in response to the shadows. Importantly, for both responses, the behavior persisted following cessation of the shadow stimuli and gradually decayed back to baseline (Figures 1E, 1F, and 1I).

### ReVSA Behaviors Scale with Shadow Number

Our initial experiments suggested a positive relationship between swipe number and the population velocity of flies (Figures 1E and 1F; Figure 2A). To investigate this relationship further, we varied systematically swipe number in a series of interleaved experiments. Cohorts of ten male flies received two, four, six, eight, or ten passes, with each pass separated by a 1-s inter-swipe interval (ISI). Delivering more shadows resulted in greater peak velocities for the flies (Figure 2B). Both the non-zero slope of the relationship between peak velocity and number of shadow passes (Figure 2D) and pairwise contrasts between peak velocities for different numbers of shadows (Figures 2E, 2F, and 3C, “passes with ISI=1 sec”) reached significance (in this and in subsequent pairwise comparisons, unless otherwise indicated, statistical significance computed by Kruskal-Wallis one-way ANOVA followed by Bonferroni-corrected pairwise Mann-Whitney U tests;  $p < .05$  for 2p versus 6p, 8p, or 10p;  $p < .01$  for 4p versus 10p). Therefore, for an ISI of 1 s, peak cohort velocity scales with shadow number.

The peak fraction of flies exhibiting hopping behavior also appeared to increase with shadow number (Figure 2C). Statistical analysis indicated that the peak probability of hopping indeed increased as a function of swipe number: there was a statistically significant non-zero slope for the relationship between peak hopping fraction and number of shadow passes (Figure 2G), and there were significant pairwise differences ( $p < .05$ ; 2p versus 8p or 10p) between peak hopping fraction for different numbers of shadows (Figures 2H, 2I, and 3E, “passes with

ISI=1 sec”). We conclude that for an ISI of 1 s, both peak velocity and the peak fraction of flies hopping increase with shadow number.

### Scaling of ReVSA Output Depends on the ISI Value

The foregoing data suggested that flies can summate the influence of multiple, closely spaced shadow stimuli to produce an increase in the magnitude of their response. The effect of this summation decays over time following stimulus offset. To investigate whether this effect might reflect an underlying “leaky” integrative process, we asked whether it was dependent on the ISI (Figures 3A and 3B). We intuited that if integration produced an accumulating internal variable with a fixed rate of decay (Figure 4A), then spacing the stimuli further apart, to increase the amount of “leakage” between each successive shadow, might prevent or reduce the cumulative response to multiple shadow stimuli.

To address this issue, we interleaved experiments in which flies received two, four, six, eight, or ten passes, respectively, under two interleaved ISI regimes. In the first regime, the ISI was set to 1 s (red, Figures 3C and 3D), whereas in the second regime, it was set to 3 s (blue, Figures 3C and 3D). Notably, a scalable increase in peak velocity was observed with an ISI = 1 s, but not for an ISI = 3 s, based on linear fittings to the data (which indicated that the slope of the ISI = 1 curve, but not the slope of the ISI = 3 curve, was significantly different from zero,  $p < .05$ ; Figure 3D). Pairwise tests indicated that there was a statistically significant increase in the response to two versus ten shadows when ISI = 1 s ( $p < .001$ ), but not when ISI = 3 s (Figures 3C, S2A, and S2B). We found a similar ISI dependence of cumulative increases in the hopping response (Figures 3E, 3F, and S2C–S2F). Hence, the scalable nature of both the locomotor and hopping responses to increasing numbers of shadow passes is dependent on the length of the ISI, with the transition point between cumulative versus non-cumulative responses under these conditions lying somewhere between ISI = 1 s and ISI = 3 s.

### A Simple Model Based on a Leaky Integrator Can Predict the Qualitative Features of ReVSA

The foregoing data strongly suggested the existence of an underlying scalable but labile quantity that accumulates in response to multiple shadows and whose integrated value is reflected in the magnitude of the ReVSA response. To investigate the behavior of such a system in a more quantitative manner, we constructed a simple mathematical model of a leaky “leaky integrator,” in which each shadow adds a constant value to the integral, and the integral value leaks at a rate proportional to its magnitude (Figures 4A and 4B; Supplemental Experimental Procedures).

This model makes different predictions according to the relative length of the ISI: (1) in a regime where the ISI is very large compared with the leak rate, there should be no accumulation (Figure 4F); (2) in a regime where the ISI is small compared with the leak rate, there should be a cumulative increase in the value of the integral as a function of stimulus number (Figures 4H and 4I); and (3) in a regime where the ISI is intermediate relative to the other two regimes, there should be a static increase relative to baseline that levels off after several shadows (Figure 4G). The experimental data provide examples of each of



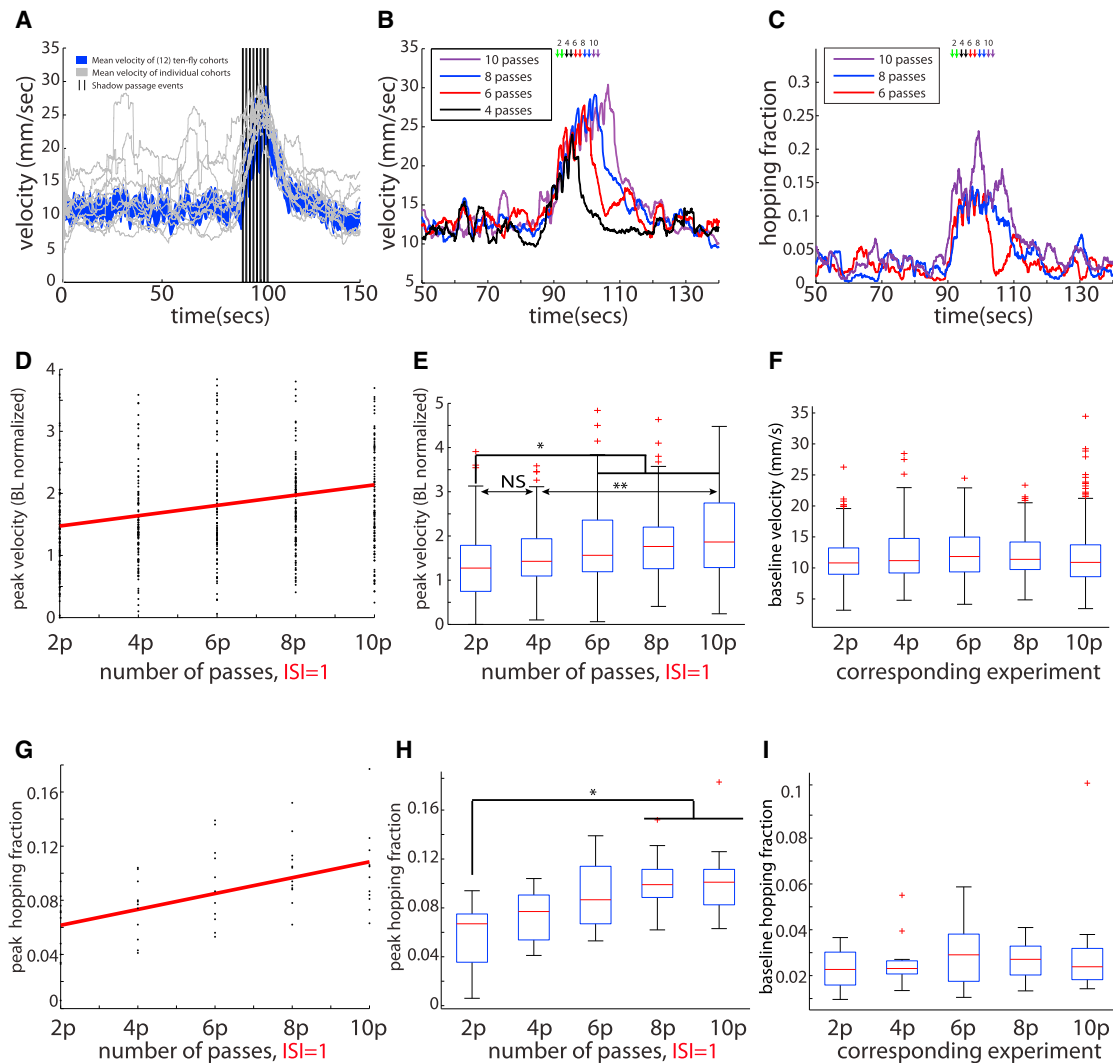


**Figure 2. For ISI = 1 s, Peak Velocity Scales with Stimulus Number**

(A) Mean velocity across 12 ten-fly cohorts (blue), with sample trajectories (gray; one per cohort) in response to shadows (black).  
 (B) The number of shadow passes (back and forth), whether 4 (black), 6 (red), 8 (blue), or 10 (purple), alters the response's peak velocity.  
 (C) The fraction of flies jumping increases with pass number: 6 (red), 8 (blue), or 10 (purple).  
 (D) Linear regression (red) for the response's peak height, when flies receive 2–10 passes (\* indicates significantly different from zero; see bottom of legend).  
 (E) Slope is non-zero (Kruskal-Wallis test), as confirmed by pairwise tests (see bottom of legend); see Figure S2A. Peak velocity, normalized to baseline, for flies receiving 2–10 passes with ISI = 1 s.  
 (F) Baselines for data in (E) are not different from each other (Kruskal-Wallis test).  
 (G) A linear regression (red) with positive slope (\*; see bottom of legend) for the fraction of hopping flies versus the number of passes received ( $p = 2$ –10).  
 (H) Pairwise tests (see bottom of legend) confirm a monotone increasing trend in the median values.  
 (I) Baseline hopping fractions are not different from each other (Kruskal-Wallis test). Total sample sizes for the two- to ten-pass experiments are, respectively, 110, 109, 108, 120, and 119 flies. Cohort sizes were 8–10 flies each.

Panels (A)–(I) reuse data from Figures 1E–1K for purposes of analysis and direct comparison. Unless otherwise indicated, in this and all subsequent main and supplemental figures, pairwise tests are Bonferroni corrected post hoc Mann-Whitney U tests following significant differences determined by Kruskal-Wallis one-way ANOVA. Asterisks represent  $p$  values, where (\*), (\*\*), and (\*\*\*) denote, respectively,  $p < .05$ ,  $p < .01$ , and  $p < .001$ . We use  $\alpha = 0.05$ . Slopes from (D) and (G) differ from zero (\*) because their 95% confidence intervals (CIs) exclude zero.

these three regimes. An ISI = 10 s corresponds to the first regime (Figures 4C and 4F); an ISI = 3 s corresponds to the intermediate regime (Figures 4D and 4G); and an ISI = 1 s corresponds to the regime that exhibits a cumulative increase in response to each shadow pass (Figures 4E and 4H). Therefore, for different ISI values that yield three qualitatively distinct response regimes,

the experimentally observed behavioral responses to successive shadow presentations can be recapitulated by a leaky integrator model. Taken together with the observation that single flies also show evidence of shadow integration (see next section), this model is consistent with an internal state change that is represented by a cumulative, labile variable.

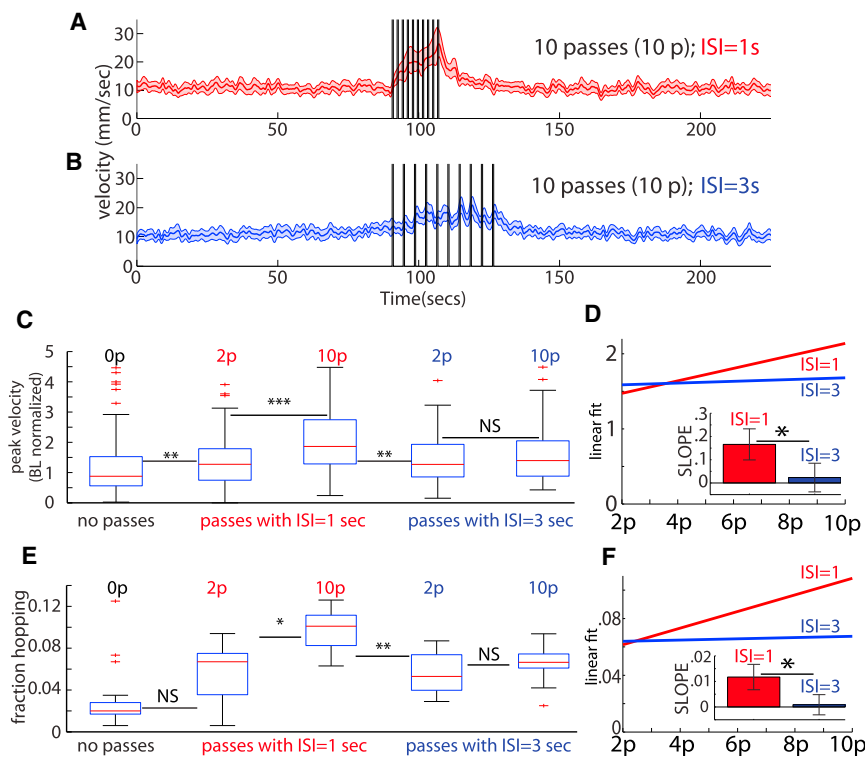


**Figure 3. Scalability in ReVSA Depends on ISI Value**

(A and B) Response to ten passes (black bars) with ISI = 1 s (red; A) or ISI = 3 s (blue; B).

(C) Peak velocity is greater (\*\*\*) following  $p = 10$  versus  $p = 2$  when ISI = 1 s (red), but not when ISI = 3 s (blue).

(D) Linear fits to the peak velocity versus  $p$  for ISI = 1 s (red) and ISI = 3 s (blue). Inset: Slopes are significantly different (\*; see bottom of legend). Slope for ISI = 1 s is positive, but for ISI = 3 s, it is indistinguishable from zero (\*; see bottom of legend).

(E) Hopping fraction is greater for  $p = 10$  versus  $p = 2$  when ISI = 1 s (\*), but not when ISI = 3 s.

(F) Linear fits to peak hopping fraction versus  $p$ , for ISI = 1 s (red) and ISI = 3 s (blue). Inset: Slope values. Slope for ISI = 1 s is positive (\*; see bottom of legend), but for ISI = 3 s, it is indistinguishable from zero. In ISI = 1 s groups, for  $p = 2-10$ , sample sizes are, respectively, 110, 109, 108, 120, and 119 flies. For the ISI = 3 s groups, for  $p = 2-10$ , sample sizes are, respectively, 100, 110, 100, 110, and 118 flies. Error bars on bar graphs represent 95% CIs. For ISI = 1 s, data in (C)–(F) are reused from Figure 2 for comparative purposes. Asterisks represent  $p$  values, where (\*), (\*\*), and (\*\*\*) denote, respectively,  $p < .05$ ,  $p < .01$ , and  $p < .001$ . Slopes from (D) and (F) differ (\*) because their 95% CIs do not overlap. Slopes for ISI = 1 have 95% CIs that exclude zero; hence, they differ (\*) from zero.

### ReVSA Output Is Scalable in Single Flies

It was formally possible that the integration process suggested by the foregoing experiments is not a property of individual flies but instead reflected a collective, population- or swarm-level integration. To test whether such integration can occur in single flies, we performed ReVSA experiments on individual animals with an ISI of 1 s and varied the number of passes (Figure 5A). As in the case of population measurements, peak velocity was measurably greater (Kruskal-Wallis test,  $p < .001$ ) after flies had received ten shadow passes as compared with only two passes (Figures 5B, 5C, and 5E), although both stimulus paradigms increased peak velocity over baseline (Figure 5D). In addition, the peak hopping fraction for single flies was also elevated relative to baseline ( $p < .001$ ), with flies exposed to ten shadows showing a trend to a higher hopping fraction than those exposed to two shadows (Figure 5F). Thus, single flies exhibit a scalable output in peak velocity according to the number of shadows delivered. To test for leaky integration in single flies, we compared the integration achieved by flies receiving ten passes with an ISI of either 1 s or 10 s. Strikingly, single flies showed greater integration when the ISI was 1 s ( $p < .001$ , Figures S4D–S4F). These data support the idea that the cumulative response to the shadows reflects an internal state that is based on leaky integration of multiple shadow stimuli.

### Single Flies Exhibit Shadow-Induced Freezing Behavior

In addition to locomotor and hopping-based behaviors, a small fraction (~30%) of animals in the single-fly experiments exhibited immobility immediately following exposure to the shadow (Figures 5G–5J and S7; Movies S2 and S7 at 45 s) to such an extent that their lack of motion could not be distinguished, at

least by eye, from a freeze frame. In order to more fully characterize this apparent “freezing” behavior in response to the shadow, we spaced the shadow passes very far apart (15 s) so as to not disturb the initial freezing posture (Figures 5G and 5H; note the frozen wing posture in Figure 5H).

To characterize this behavior more quantitatively, we built a semi-automated freezing classifier based on pixel movement (see Experimental Procedures) [48]. Frame to frame, we find statistically significant enrichment for freezing behavior ( $p < .001$ ), relative to baseline, immediately following the first shadow, and also the second shadow ( $p < .001$ ), although the first shadow’s enrichment is much greater (Figures 5I and 5J). Moreover, there is a significant cross-correlation ( $p < .05$ ) between the shadow’s presence and subsequent freezing (Figure S7G). We conclude that the freezing behavior is caused by the shadow and is not simply due to spontaneous bouts of inactivity. This behavior, which is here shown to occur in response to an ecologically relevant stimulus, is reminiscent of the freezing responses observed in rodents and other animals in response to threats [49, 50]. An immobility behavior in *Drosophila* has been reported previously in response to translational motion of a small fly-sized robot moving in the same plane as the fly [51]. In contrast, the shadow stimulus used here is designed to mimic a threat from an aerial predator. Given these differences, it is difficult to ascertain whether the previously reported behavior is identical to the freezing described here.

### An Overhead Shadow Interrupts Feeding Behaviors in Starved Flies

The foregoing experiments suggested that multiple shadow presentations can induce a persistent state of hyperactivity, similar

to the persistent response to multiple air puffs in the ReSH assay [20]. In principle, hyperactivity may have a positive or negative valence; for example, flies increase their locomotor velocity in response to ethanol, which is rewarding [34, 52]. To investigate whether the ReVSA response has a negative valence, we tested whether the shadow stimulus can interfere with an appetitive behavior, specifically feeding, which is highly sensitive to disruption by threats [53–56]. To this end, we introduced starved flies into a modified version of the chamber in which a food patch was placed in the center (Figure 6A) and onto which they quickly congregated (Figures 6B and 6D; “loading onto food”).

While aggregated on the food patch, flies ( $n = 10$  per assay) were subjected to a series of overhead shadows. In response to the shadow, the flies mostly did not jump but rather stopped feeding and walked off the food onto the surrounding plastic (Movie S5). On average, with each passing shadow, more and more flies left the food patch, a behavior recapitulated by single flies (Figures 6C, S3A, S3B, S3L, and S3M; Movie S7). Once off the food patch, the flies continued to respond to the shadow (Movie S5; Figures S3I–S3K). Very starved (27.5–30 hr food deprivation) animals were harder to disperse from the food (i.e., required more shadow passes) than were less starved (24–27.5 hr food deprivation) animals, suggesting that feeding and escape are competing behaviors. Fed flies investigating decapitated virgin females were also dispersed less effectively by the shadow (data not shown), suggesting that the sensitivity to the shadow is influenced by the relative strength or salience of a competing appetitive stimulus. Finally, when larger numbers of shadows ( $\sim 20$ ) were delivered with sufficiently long ISIs (10–20 s), the flies showed evidence of habituation (Figures S4A–S4C). Anecdotal observations indicated that flies habituated to the shadow could be dishabituated using a mechanical startle stimulus (Movie S4), providing evidence of cross-modal control of this state.

In some experiments (Figures S3L and S3M), no flies left the food in response to the first pass of the shadow and only began to disperse following the second or third shadow exposure, suggestive of sensitization (see also Figure S3F; Movie S7, part 3). Interestingly, this increasing responsiveness to the shadow following multiple passes was only observed if the time delay between the excursion and return of the shadow paddle was sufficiently short (Figures S5E–S5G). This is consistent with the model of an internal leaky integrator that controls the magnitude of the shadow response (Figure 4). Thus, the response to the shadow on the food patch shows evidence of integration, as is the case for flies tested in the absence of food (see above).

The observation that feeding is interrupted by the shadow suggests that the shadow has a negative valence. Several other lines of evidence support this interpretation. First, flies avoided the paddle’s path when it was presented in a manner that covered only half the arena (Figures S6A–S6C). Second, high-resolution video analysis demonstrated that flies moved away from the paddle’s direction of motion (Figures S6D–S6G; Movie S6). Together, these data argue that the shadow response has a negative valence. Moreover, the fact that the shadow does not simply produce an increase in locomotion, as observed in the absence of food (Figures 1, 2, and 3), but that it also produces radial dispersal from a food resource (Figure 6), suggests that

the ReVSA response exhibits flexibility and can generalize to a different context.

### Time to Return to the Food Patch Increases with the Number of Shadow Passes

Anecdotally, when animals are dispersed from a food resource (e.g., birds from a feeder) by a predator or other threat, there is often a delay before they return to the resource. Similarly, for the case of the ReVSA food-based assay, we observed in both cohorts of animals and in single flies that, once dispersed from the central food resource by multiple (four) shadows, animals showed a significant time delay before returning to the food (Figures 6C and S3A; Movie S5). This delayed return suggests that the shadow’s effect persists, in some cases for minutes, after the flies have left the food. This observation suggests that the flies may enter a state of persistent defensive or threat arousal upon exposure to multiple shadows and that this labile state may compete with the animals’ drive to return to the food, until it decays below a certain threshold.

If the labile state is indeed produced by a leaky integrator of shadow exposure, then one would predict that dispersing the flies with a greater number of shadows ( $>4$ ) would lengthen the time to return to the food patch because the integrated value of the state would initially be higher following stimulus offset. To test this prediction, we introduced cohorts of 7–10 starved flies into the arena and allowed them to load onto the food patch (Figure 6D; from 0–90 s). At 90 s, we delivered either four passes of the shadow or ten passes of the shadow, in each case with a 1-s ISI. For these experiments, we chose an empirically determined shorter starvation period, such that most or all flies would be dispersed by only 1–2 shadows (Figure 6D). This eliminated confounds due to difference in total food consumption between the four- versus ten-shadow conditions.

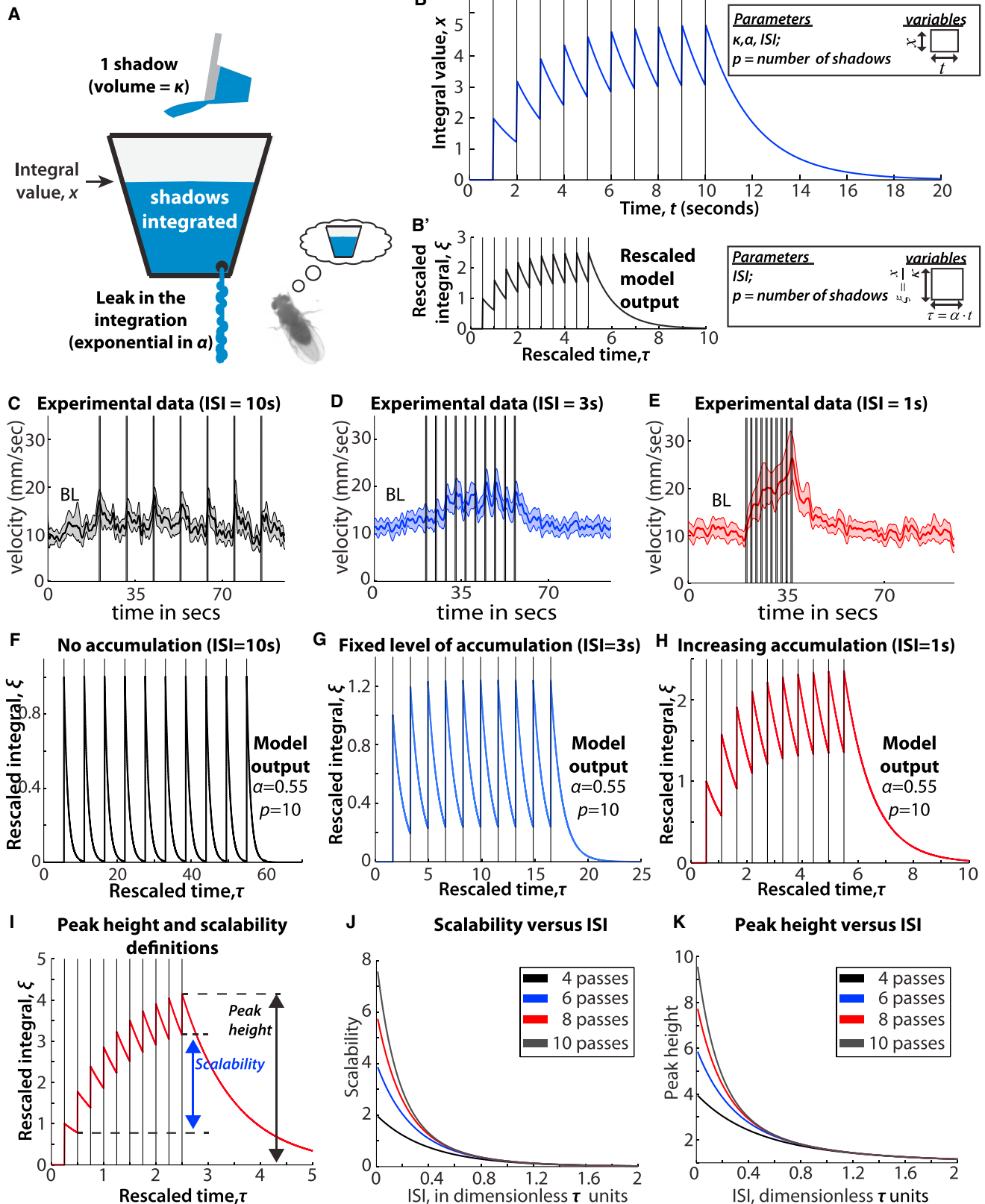
Strikingly, the return kinetics were slower for flies exposed to ten passes of the shadow, compared with flies returning after only four passes of the shadow (Figure 6D; “post-shadow return to food” region). Quantitatively, an exponential fit to the return curve of flies off food as a function of time (Figure 6E) revealed a significant difference ( $p < .05$ ) in return kinetics as a function of swipe number. We conclude that flies dispersed from a food resource take longer to return to the resource when the number of shadows used for dispersal is larger.

### Can the Delayed Return to Food Reflect Thigmotaxis or Initial Distance from the Patch?

Once flies are dispersed from the food, it is possible that other non-defensive competing behaviors executed by the animals might delay their return to the food patch. One such behavior is thigmotaxis, in which animals move at a roughly constant velocity along the perimeter of the walking arena. We observed that following dispersal from the food in response to the shadow, some of the flies indeed engaged, at least transiently, in thigmotaxis. This thigmotactic behavior could reflect a continued drive to escape the arena, due to the persistent defensive state caused by the shadow (similar to anxiety behavior in the open field test used in rodent models [57]). Alternatively, it could be due to a self-reinforcing behavioral “attractor” reflecting a psychophysical phenomenon, such as maximizing retrogressive movement on the retina.



## Simple model of shadow integration



(legend on next page)

We therefore investigated whether an increase in thigmotaxis could be responsible for the slower return to food in the cohort exposed to ten versus four shadows. We first quantified thigmotaxis for both cohorts. The level of thigmotaxis was low (<20%) because the arena walls were covered with SigmaCote and was only marginally different for flies in the ten- versus four-pass cohorts (Figure 6F). Nevertheless, to eliminate any contribution of thigmotaxis, we re-analyzed the data, eliminating any flies that were in thigmotaxis at any given time point. Even with this stringent filter, the return kinetics were still significantly slower ( $p < .05$ ) for the ten-shadow cohorts than for the four-shadow cohorts, as verified by exponential curve fitting and decay constant analysis (see Figure 6G, inset). We conclude that the slower return to food of flies exposed to ten-shadow stimuli is unlikely due to a relative increase in thigmotaxis, whether or not this behavior reflects an underlying anxiety-like state or a psychophysical attractor.

Finally, we investigated whether the ten-shadow cohorts took longer to return to the food simply because they were initially dispersed further from the patch than were the four-shadow cohorts, following shadow stimulus termination. Although flies in the ten-shadow cohort were indeed distributed a few millimeters further from the food patch (Figure 7A), even after normalizing for this initial difference, their return kinetics to the food patch were slower ( $p < .05$ ; Figure 7A, inset, “rescaled data” and Figure 7B). Together, these analyses eliminate differences in thigmotaxis, or post-shadow dispersal radius, as being responsible for the slower return to the food patch by flies exposed to ten- versus four-shadow stimuli. More likely, the difference reflects a higher initial level and therefore a longer decay time, for a shadow-induced defensive state, which competes with the flies’ appetitive drive to return to the food. Consistent with this interpretation, the flies exposed to ten shadows took longer to “calm down” following the stimulus ( $p < .05$ ), as determined by the post-shadow decay kinetics of both velocity and fraction hopping (Figures 7C and 7D). This may be due to the fact that those flies were exposed to more shadows after they had left the food (Figure 6D) since the response to the shadow off the food was more vigorous than when the flies were on the food (Figures S3I–S3K).

## DISCUSSION

Defensive responses to threats involve both rapid, reflex reactions and (in higher organisms) more sustained, state-dependent

“integrative” behavioral responses. The former are likely to have evolved before the latter, as they are exhibited even by unicellular organisms. The latter type of response can reflect an internal arousal or emotion state; humans subjectively experience and report such a threat state as “fear” or “anxiety” [15]. When such integrative responses to threats first began to emerge in evolution and whether they involve neural circuits overlapping with, or distinct from, those mediating reflexive responses is not known. Flies are well known to exhibit rapid, reflexive jump responses to a single presentation of a looming shadow [37–39] (but see [58]). However, whether they are also capable of exhibiting longer-term, integrated responses to repetitive shadow stimuli has not been investigated previously.

Here, we describe a novel behavioral assay, called ReVSA, in which flies can be exposed to repeated presentations of an aversive shadow stimulus in an enclosed arena, preventing escape. Under these conditions, we observe features of the behavioral response that are suggestive of an internal state exhibiting multiple emotion primitives [3]. First, the response exhibits persistence: flies exposed to repeated shadow stimuli remain active for tens of seconds after the stimulus has terminated. Second, the response exhibits a negative valence, in that it interferes with feeding and that flies avoid the moving shadow in a directional manner. Third, the response generalizes across multiple settings (freely moving flies on plastic; stationary feeding flies on a food patch). Fourth, the response exhibits “stimulus degeneracy”: a similar persistent increase in locomotor hyperactivity can be elicited by repeated presentation of a mechanical startle stimulus [20]; moreover, flies habituated to the shadow stimulus can be dishabituated by a mechanical startle. Finally, and most importantly, the behavioral response scales with stimulus number and frequency. These behavioral responses suggest that the response to multiple shadows reflects an underlying causal [3, 4] internal state characterized by the emotion primitives described above.

This inferred state can be mathematically modeled by assuming a shadow-induced labile quantity that accumulates with repeated shadow stimuli—in other words, a leaky integrator [59] of shadow exposure. We emphasize that this model is simply a formalized illustration, and not a curve-fitting exercise. Nevertheless it may provide a useful heuristic for designing future experiments. Our model bears some resemblance to the “hydraulic” metaphor proposed by Lorenz [60, 61] to explain how internal drive or motivational states influence behavior, with some

### Figure 4. A Leaky Integrator of Shadow Exposure

(A) Cumulative shadow integral is analogous to the water level in a reservoir. Shadows (cups of water) fill the reservoir, whereas a slow leak drains the reservoir. (B) Model output (blue), with shadow passes (black lines). Model parameters are as follows:  $\kappa$ , the fill rate;  $\alpha$ , the leak rate;  $p$ , pass number, which is the number of shadows received; and the ISI. Variables (inset) are time,  $t$ , and the reservoir’s fill level,  $x$ . (B’) Rescaled model output (black), which eliminates redundant parameters to simplify analysis (see Supplemental Experimental Procedures). The parameters for the rescaled model are pass number,  $p$ , and the ISI. Variables (inset) are  $\tau = t \cdot \alpha$  and  $\xi = x / \kappa$ . See Supplemental Experimental Procedures for detailed explanation. (C–E) Experimental time series data for ISI = 10 s, ISI = 3 s, and ISI = 1 s. (F–H) Model output ( $\alpha = 0.55$ ). (F) When ISI = 10 s, the reservoir completely empties between passes, as in (C). (G) When ISI = 3 s, the integral saturates after only a few passes, as in (D). (H) When ISI = 1 s, the integral increases, as in (E). (I) Diagram illustrating scalability and peak height definitions (see Supplemental Experimental Procedures). (J) Scalability versus pass number,  $p$ , and ISI. (K) Peak height versus  $p$  and ISI. Data from (D) and (E) are from Figures 3A and 3B. Sample sizes for (D)–(F) are 105, 118, and 119 flies.

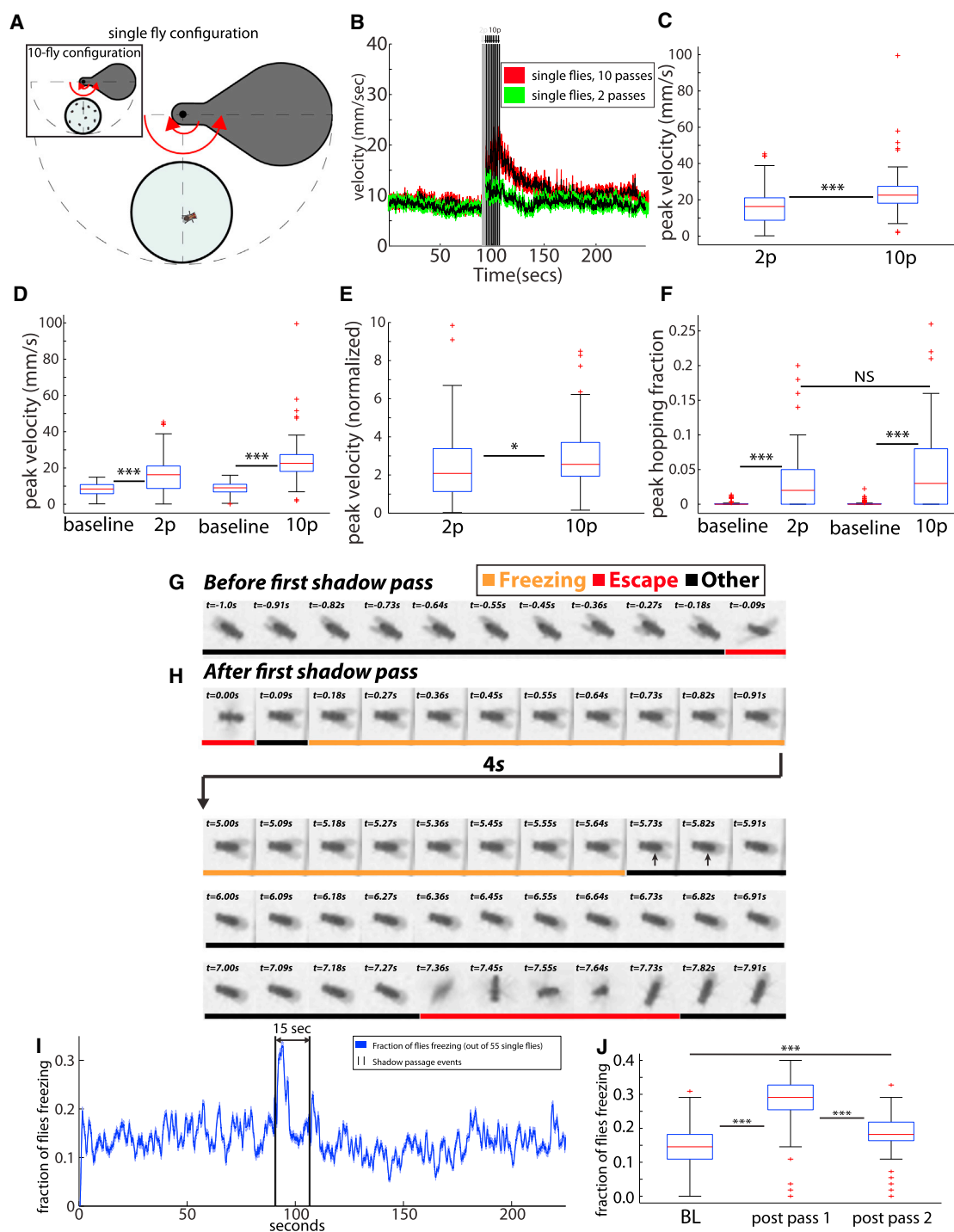


**Figure 5. Single-Fly ReVSA Dynamics Recapitulate Group Dynamics and Include Freezing Behaviors**

(A) Single-fly ReVSA assay.  
 (B) Time course for single-fly velocities. For pass number  $p = 10$  (red envelope, black curve), the peak velocity is greater, and it persists longer, than for  $p = 2$  (green envelope, black curve).  
 (C) Peak velocity for  $p = 10$  is significantly greater than for  $p = 2$  (\*\*\*, Kruskal-Wallis test).  
 (D) Peak velocities differ from baseline and increase with  $p$  (\*\*\*).  
 (E) Peak velocity for  $p = 10$  is still greater than  $p = 2$  when normalized to baseline (\*, Kruskal-Wallis test).  
 (F) Peak hopping fraction for  $p = 10$  trends toward being greater than  $p = 2$ ; both values differ significantly from baseline (\*\*\*).  
 (G) Kymograph prior to the first pass (orange for freezing, red for escape, and black for other).  
 (H) Kymograph after the first pass.  
 (I) Fraction of flies freezing (out of 55 single flies).  
 (J) Fraction of flies freezing for BL, post pass 1, and post pass 2.

(legend continued on next page)

important differences. First, in Lorenz's metaphor the "drive"-filled vessel did not leak; it simply discharged its contents when a given behavior was released. Second, the level of drive was internally generated, whereas in the present case, it is generated by an external sensory (visual) stimulus. Similar effects can be produced with a noxious mechanosensory stimulus [20]. In honey bees, alarm pheromones [62] can induce persistent states of arousal; therefore, pheromones likely can induce such defensive internal states as well.

The circuit-level mechanisms underlying such a leaky integrator remain to be investigated; multiple implementations are possible [63], including both network-based and molecular instantiations. Neuromodulators, such as biogenic amines or neuropeptides, are attractive candidates for the latter class of mechanism because they could encode scalability by their concentration and persistence by their rate of clearance. Indeed, across phylogeny, some neuropeptides are strikingly well conserved in their behavioral roles [64]. Biogenic amines such as dopamine also play a conserved role in arousal [20, 65]. *Drosophila* as a genetic system is particularly well suited to search for such molecular mechanisms [66]. Leaky integrators can also be instantiated by a number of circuit-level mechanisms [63]. Improvements in population measurements of neural activity in head-fixed flies may aid in their discovery. Visual stimuli are vastly preferable to mechanical (startle) stimuli for such studies [58] because the stimulus itself does not physically perturb the flies.

What is the adaptive value of a system that integrates multiple threat stimuli to produce a scalable defensive response? Isn't it safer for the fly simply to jump away as soon as it sees an overhead shadow? That may be the case for a well-fed fly, but starved flies engaged in feeding must make a cost-benefit decision: premature flight from a resource deprives the animals of food and consumes energy; conversely, delayed escape renders the animals increasingly vulnerable to predation. The ability to encode an integrated, scalable internal representation of the history of recent threats (which may share some features with working memory [67]) and to use that representation to select behavioral responses and to tune their intensity may be adaptive in uncertain environments. Whether this depends on the predictability of the shadow remains to be investigated. In addition, our data suggest that these integrated responses may be reinforced or "sharpened" by social interactions: flies feeding in groups are less readily dispersed by the first shadow than are single flies (Figures S3A and S3C), and return to food following dispersal is faster than for single flies (Figures S3G and S3H), suggestive of cooperativity.

The behavioral response of flies in the ReVSA assay exhibits multiple properties consistent with the expression of a persistent, internal defensive state, possibly an evolutionary precursor to the emotion that humans subjectively experience as "fear." Interestingly, recent studies in mice have shown that optogenetic stimulation of the ventromedial hypothalamus can elicit

defensive behaviors exhibiting a similar set of properties [43, 44]. The establishment of this paradigm in *Drosophila* opens the way to a mechanistic dissection of the molecular and circuit-level implementation of this state, in a genetically powerful invertebrate species. Such mechanistic studies should help to resolve the long-standing issue of the causal relationship between behavior and internal emotion states [4, 7] and may also shed light on the phylogenetic origins and continuity of emotion.

## EXPERIMENTAL PROCEDURES

### Animal Husbandry

Male flies were raised on Caltech brown food at 25°C at 55% humidity. Flies used for experiments were 5–7 days old, with all experimental and control cohorts matched for age, genetic background, and husbandry conditions.

### Fly Strains

Experiments were performed in a w+ genetic background. We used a hybrid background between the Janelia Farm attp2 landing site flies (which were the paternal flies) and *Canton S* (which were the maternal flies), except in Figures S1, S3, S4, S6, S7, and 6C and Movies S4, S5, and S7, which used *Canton S* flies.

### Starvation Protocols

Animals in food experiments were wet starved for 24–30 hr, with slight adjustments in starvation length (matched for experimental and control animals) to ensure that animals could load onto food within a ~90-s time window. Animals in non-food experiments were wet-starved for 16–24 hr, except for the case of single-fly experiments, which used non-starved animals.

### Fly Detection and Tracking

Flies were filmed using a Point Grey grasshopper camera (part # GRAS-03k2m/c) against an Advanced Illumination backlight (part # BL0608-880-IC). Pixels belonging to flies were detected by background subtraction and then merged and segmented using custom-built machine vision software. Fly identities were tracked between frames using the Hungarian algorithm. Velocity measurements are computed in terms of fly centroids.

### Control of Paddle Motion

We used a custom-built control algorithm for programming paddle movements, which were controlled in terms of a MATLAB graphical user interface, also custom-built.

### Dwell Time Convention

For all experiments discussed in this paper (except Figures 5I and S6, which deliberately varied the dwell time for a single excursion and return of the paddle), we took the dwell time to be equal to the ISI, thus producing a stimulus that appears at regular intervals.

### Acclimatization to the Chamber

Flies were acclimatized to the chamber for at least 90 s prior to the first shadow stimulus.

### Chamber Geometry

The behavioral chamber is about 100 mm in diameter and approximately 5 mm in height, from floor to ceiling.

### Criteria for Hopping

Forward versus backward paddle experiments (Figure S1) exhibit qualitatively different log-velocity histograms (data not shown). We set a hopping velocity

(H) Kymograph following first shadow pass. Most time is spent freezing (orange label). Long arrow from  $t = 0.91$  to  $t = 5.00$  s represents 4 s of freezing. After freezing, the fly escapes (red label).

(I) Proportion of flies freezing versus time (see Experimental Procedures). Proportion freezing spikes following the first shadow.

(J) Shadow-induced elevation in the freezing rate (\*\*\*).

For panels (B)–(F), the sample size is  $n = 81$  for each condition. Sample sizes for panels (I) and (J) are  $n = 55$  single flies. See also Movie S2.

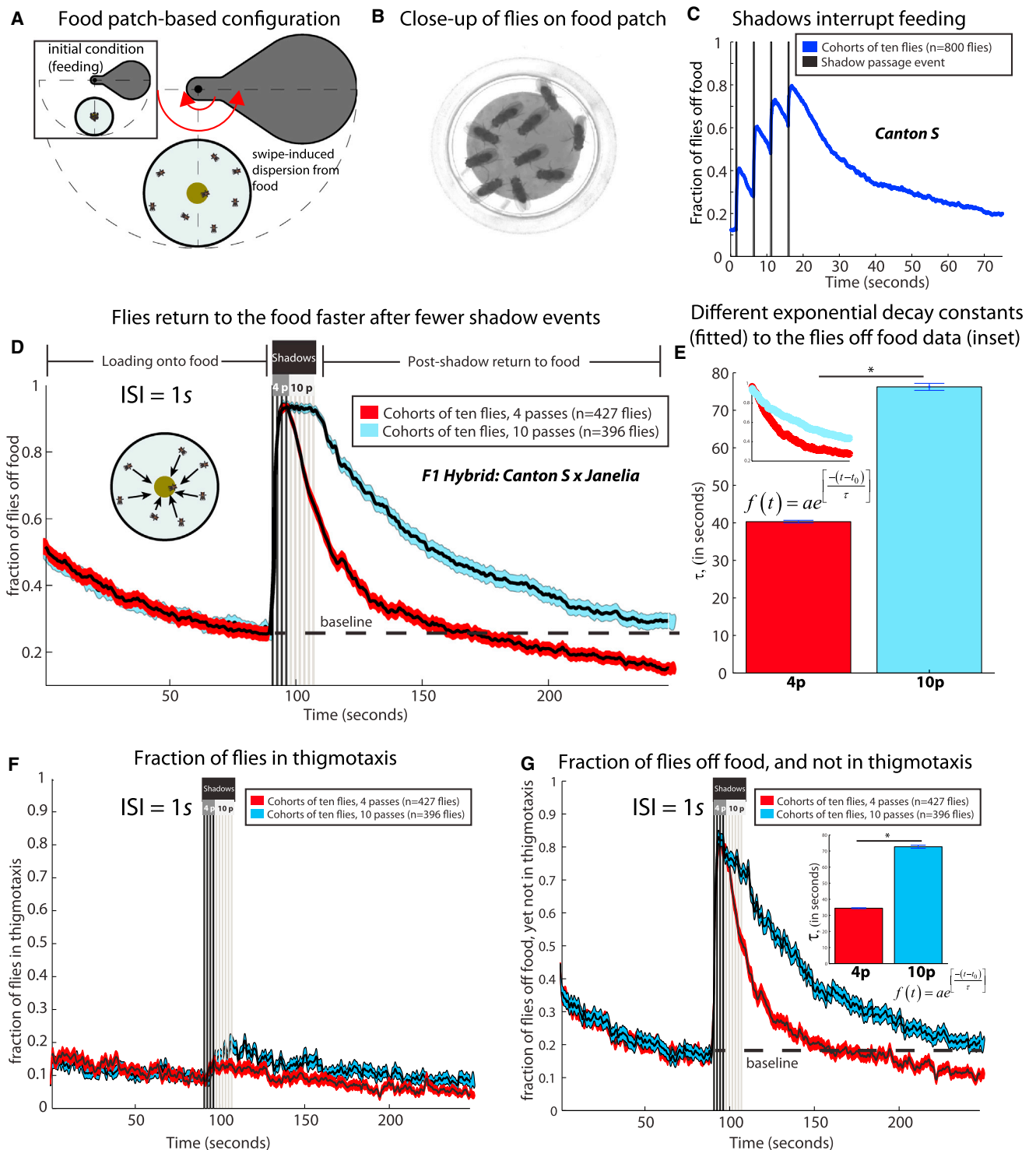


**Figure 6. Return Times in Food-Based ReVSA Assay Scale with Shadow Number**

(A) Food-based version of the assay, with a central food cup at the arena's center.

(B) Flies feeding on the food cup.

(C) Shadow passes cause starved *Canton S* flies (n = 810 flies in 81 cohorts) to leave the food, with more flies leaving at each successive pass.

(D and E) Despite identical "loading onto food" kinetics (red and blue enveloped curves), flies return to the food faster when they receive fewer shadows (pass number p = 4, black versus p = 10, gray; ISI = 1 s). The "post-shadow return to food" region of the plot shows different kinetics of return for the two different pass treatment groups. Flies receiving four passes drop below baseline, whereas the ten-pass cohorts never reach baseline. The case p = 4 has a steeper decay function than the case p = 10 (E), which is statistically significant (\*; see bottom of legend).

(legend continued on next page)



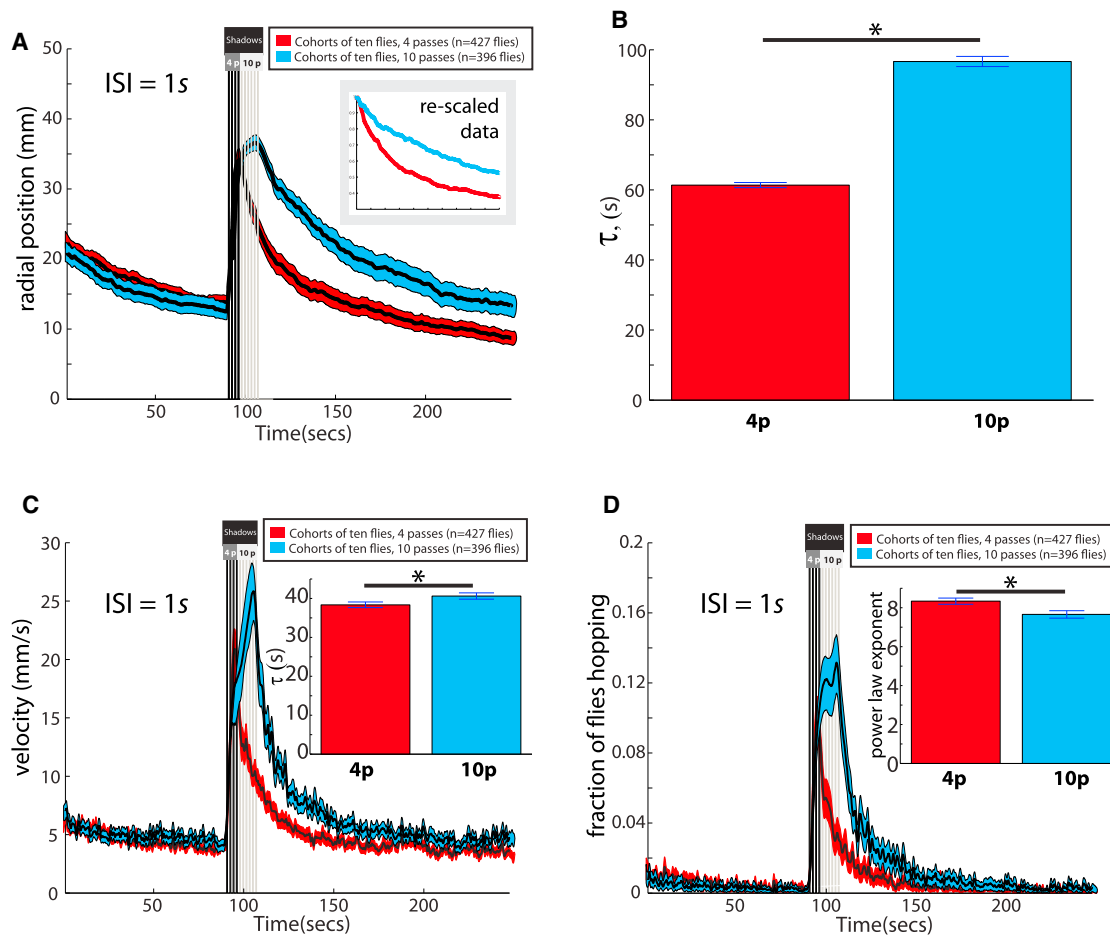


**Figure 7. Dynamics of Radial Dispersal, Velocity, and Hopping in Food-Based ReVSA Assay**

(A) Radial dispersal of flies from food. Flies receiving ten passes of the shadow are initially slightly further from the center than flies that receive four passes of the shadow, but the return kinetics are different based on rescaling (inset) or an exponential fit to the data (B).

(B) Tau values for the  $p = 10$  and  $p = 4$  pass conditions (\*; see bottom of legend).

(C) When  $p = 10$  (blue envelope), there is a higher peak velocity and slower decay (\*; see bottom of legend) than when  $p = 4$  (C, inset).

(D) Hopping frequency returns to baseline more quickly (\*; see bottom of legend; based on a power-law fit to the decay region of the function; D, inset) when flies receive four versus ten passes of the shadow.

Sample sizes for (A)–(D) are all  $n = 46$  experiments for the four-pass scenario;  $n = 46$  experiments for the ten-pass scenario. Each experiment contains 7–10 flies. Panels in Figure 7 are computed from the same dataset as panels in Figures 6D–6G. Decay constants in (B), (C), and (D) differ (\*) because their 95% CIs do not overlap. Error bars on bar graphs represent 95% CIs.

threshold above a discontinuity in the population-level log velocity, which closer investigation found corresponded to the hopping behavior. This method was validated using graphical user interface (GUI)-based manual scoring.

#### Criteria for Freezing

A fly in a given time step was considered to be freezing if its 0.98 quantile of pixel motion was below a pixel motion threshold of four gray levels per frame. Once freezing events were classified frame to frame, we re-classified freezing in terms of freezing bouts, which are given in the relevant figure panels. Unless otherwise specified (e.g., Figures 1L and S8), freezing is given as a frame-to-frame proportion.

#### Control of Paddle Motion

We used custom-made software in MATLAB to control the paddle's position. Paddle motion consisted of excursions from 0 to  $\pi$  radians (Figure 1C, clockwise arrow) and return movements from  $\pi$  radians back to 0 (Figure 1C, counterclockwise arrow), at a velocity of approximately 4.2 radians per second. We chose the paddle velocity to maximize startle effects. Paddle movements were controlled in terms of three parameters: (1) angular velocity; (2) paddle dwell time (DT), defined to be the time elapsed between excursion completion and return initiation (Figure 1D); and (3) the inter-swipe interval (ISI), defined to be the time between the previous return completion and the next excursion initiation (Figure 1D). Together, these control parameters permitted synthesis of diverse shadow stimuli.

(F) Thigmotaxis is rare whether  $p = 4$  or  $p = 10$ .

(G) Subset of flies off the food, and not in thigmotaxis, also shows a statistically significantly steeper (\*; see bottom of legend) decay for  $p = 4$  than for  $p = 10$ , suggesting that thigmotaxis is not responsible for the decay rate difference. Error bars on bar graphs represent 95% CIs.

Sample sizes for panels (D)–(G) are all  $n = 46$  experiments for  $p = 4$  and for  $p = 10$ . Decay constants in (E) and (G) are different (\*) because their 95% CIs do not overlap.

### Statistical Tests

Unless otherwise specified, a Kruskal-Wallis one-way ANOVA was used to assess whether any groups were significantly different. If differences could be detected, we then used pairwise Mann-Whitney U tests, which were corrected for multiple comparisons using the Bonferroni method. Asterisks represent p values: one asterisk (\*) denotes  $p < .05$ ; two asterisks (\*\*) denote  $p < .01$ ; and three asterisks (\*\*\*) denote  $p < .001$ . We use an  $\alpha = 0.05$  level of confidence.

### SUPPLEMENTAL INFORMATION

Supplemental Information includes Supplemental Experimental Procedures, seven figures, and seven movies and can be found with this article online at <http://dx.doi.org/10.1016/j.cub.2015.03.058>.

### AUTHOR CONTRIBUTIONS

W.T.G., M.R.M., R.R.D., C.F., P.D.F., P.P., and D.J.A. performed research. D.J.A. performed the original, food-based pilot studies of the shadow response assay in Martin Heisenberg's laboratory and at Janelia Farm and commissioned the construction of the original shadow paddle apparatus at Janelia Farm. M.R.M. built the tracker, which was modified by P.D.F. under the supervision of P.P. T.T. built the original prototype for the shadow response apparatus. L.R. designed the custom software used to control the apparatus. W.T.G. performed the majority of the experiments discussed in this paper and did the majority of the modeling and analysis used in the paper, based on an initial model of a leaky integrator made by P.P. W.T.G., M.R.M., P.P., and D.J.A. designed research. W.T.G. built the apparatus used for these experiments, with engineering support from Caltech and Janelia Farm/HHMI. W.T.G., C.F., and M.R.M. programmed scripts for computational analysis of the data. D.J.A. and P.P. supervised research. W.T.G. and D.J.A. wrote the paper.

### ACKNOWLEDGMENTS

We thank Allan Wong, Brian Duistermars, Kiichi Watanabe, Hidehiko Inagaki, Barret Pfeiffer, Prabhat Kunwar, Moriel Zelikowsky, Weizhe Hong, and Kenta Asahina for helpful comments and discussion. We also thank Gerald M. Rubin and Kevin Moses for financial support. Although all data in the manuscript were collected at Caltech, this project was initiated under the Janelia Farm Visiting Scientist Program, which provided funds for the initial prototype of the instrumentation and for associated software development. We are grateful to HHMI, NIH, and the Gordon and Betty Moore Foundation for financial support. This work was supported in part by NIH grant RO1-DA031389. W.T.G. is a fellow of the Jane Coffin Childs Foundation for Medical Research. We thank J.L. Anderson for comments on the model.

Received: December 9, 2014

Revised: March 3, 2015

Accepted: March 30, 2015

Published: May 14, 2015

### REFERENCES

- Simon, H.A. (1967). Motivational and emotional controls of cognition. *Psychol. Rev.* 74, 29–39.
- Sloman, A., and Croucher, M. (1981). Why robots will have emotions. *Proceedings of the Seventh International Joint Conference on Artificial Intelligence*, 197–202.
- Anderson, D.J., and Adolphs, R. (2014). A framework for studying emotions across species. *Cell* 157, 187–200.
- Darwin, C. (1872). *The Expression of the Emotions in Man and Animals*. (London: J. Murray).
- Oatley, K., and Johnson-Laird, P.N. (1987). Towards a cognitive theory of emotions. *Cogn. Emot.* 1, 29–50.
- Cannon, W.B. (1927). The James-Lange theory of emotions: a critical examination and an alternative theory. *Am. J. Psychol.* 39, 106–124.
- James, W. (1884). II.—What is an emotion? *Mind* 9, 188–205.
- Salzman, C.D., and Fusi, S. (2010). Emotion, cognition, and mental state representation in amygdala and prefrontal cortex. *Annu. Rev. Neurosci.* 33, 173–202.
- Iliadi, K.G. (2009). The genetic basis of emotional behavior: has the time come for a *Drosophila* model? *J. Neurogenet.* 23, 136–146.
- Döring, T.F., and Chittka, L. (2011). How human are insects, and does it matter. *Formos. Entomol.* 31, 85–99.
- Mendl, M., Paul, E.S., and Chittka, L. (2011). Animal behaviour: emotion in invertebrates? *Curr. Biol.* 21, R463–R465.
- Panksepp, J. (2005). Affective consciousness: core emotional feelings in animals and humans. *Conscious. Cogn.* 14, 30–80.
- Adolphs, R. (2010). Emotion. *Curr. Biol.* 20, R549–R552.
- LeDoux, J. (2012). Rethinking the emotional brain. *Neuron* 73, 653–676.
- Adolphs, R. (2013). The biology of fear. *Curr. Biol.* 23, R79–R93.
- Panksepp, J. (1998). *Affective Neuroscience*. (New York: Oxford University Press).
- Bateson, M., Desire, S., Gartside, S.E., and Wright, G.A. (2011). Agitated honeybees exhibit pessimistic cognitive biases. *Curr. Biol.* 21, 1070–1073.
- Fossat, P., Bacqué-Cazenave, J., De Deurwaerdère, P., Delbecq, J.P., and Cattaert, D. (2014). Comparative behavior. Anxiety-like behavior in crayfish is controlled by serotonin. *Science* 344, 1293–1297.
- Panksepp, J. (1982). Toward a general psycho-biological theory of emotions. *Behav. Brain Sci.* 5, 407–422.
- Lebestky, T., Chang, J.S.C., Dankert, H., Zelnik, L., Kim, Y.C., Han, K.A., Wolf, F.W., Perona, P., and Anderson, D.J. (2009). Two different forms of arousal in *Drosophila* are oppositely regulated by the dopamine D1 receptor ortholog DopR via distinct neural circuits. *Neuron* 64, 522–536.
- Wolf, F.W., Eddison, M., Lee, S., Cho, W., and Heberlein, U. (2007). GSK-3/Shaggy regulates olfactory habituation in *Drosophila*. *Proc. Natl. Acad. Sci. USA* 104, 4653–4657.
- Cho, W., Heberlein, U., and Wolf, F.W. (2004). Habituation of an odorant-induced startle response in *Drosophila*. *Genes Brain Behav.* 3, 127–137.
- Jordan, K.W., Morgan, T.J., and Mackay, T.F.C. (2006). Quantitative trait loci for locomotor behavior in *Drosophila melanogaster*. *Genetics* 174, 271–284.
- Yamamoto, A., Zwarts, L., Callaerts, P., Norga, K., Mackay, T.F.C., and Anholt, R.R.H. (2008). Neurogenetic networks for startle-induced locomotion in *Drosophila melanogaster*. *Proc. Natl. Acad. Sci. USA* 105, 12393–12398.
- van Swinderen, B., Nitz, D.A., and Greenspan, R.J. (2004). Uncoupling of brain activity from movement defines arousal States in *Drosophila*. *Curr. Biol.* 14, 81–87.
- Nitz, D.A., van Swinderen, B., Tononi, G., and Greenspan, R.J. (2002). Electrophysiological correlates of rest and activity in *Drosophila melanogaster*. *Curr. Biol.* 12, 1934–1940.
- Krashes, M.J., DasGupta, S., Vreede, A., White, B., Armstrong, J.D., and Waddell, S. (2009). A neural circuit mechanism integrating motivational state with memory expression in *Drosophila*. *Cell* 139, 416–427.
- Waddell, S. (2010). Dopamine reveals neural circuit mechanisms of fly memory. *Trends Neurosci.* 33, 457–464.
- Waddell, S. (2013). Reinforcement signalling in *Drosophila*; dopamine does it all after all. *Curr. Opin. Neurobiol.* 23, 324–329.
- Liu, C., Plaçais, P.Y., Yamagata, N., Pfeiffer, B.D., Aso, Y., Friedrich, A.B., Siwanowicz, I., Rubin, G.M., Preat, T., and Tanimoto, H. (2012). A subset of dopamine neurons signals reward for odour memory in *Drosophila*. *Nature* 488, 512–516.
- Burke, C.J., Huetteroth, W., Oswald, D., Perisse, E., Krashes, M.J., Das, G., Gohl, D., Silles, M., Certel, S., and Waddell, S. (2012). Layered reward signalling through octopamine and dopamine in *Drosophila*. *Nature* 492, 433–437.
- Heisenberg, M. (2003). Mushroom body memoir: from maps to models. *Nat. Rev. Neurosci.* 4, 266–275.

33. Shohat-Ophir, G., Kaun, K.R., Azanchi, R., Mohammed, H., and Heberlein, U. (2012). Sexual deprivation increases ethanol intake in *Drosophila*. *Science* 335, 1351–1355.
34. Kaun, K.R., Azanchi, R., Maung, Z., Hirsh, J., and Heberlein, U. (2011). A *Drosophila* model for alcohol reward. *Nat. Neurosci.* 14, 612–619.
35. Yang, Z., Bertolucci, F., Wolf, R., and Heisenberg, M. (2013). Flies cope with uncontrollable stress by learned helplessness. *Curr. Biol.* 23, 799–803.
36. Maier, S.F., and Watkins, L.R. (2005). Stressor controllability and learned helplessness: the roles of the dorsal raphe nucleus, serotonin, and corticotropin-releasing factor. *Neurosci. Biobehav. Rev.* 29, 829–841.
37. Card, G., and Dickinson, M.H. (2008). Visually mediated motor planning in the escape response of *Drosophila*. *Curr. Biol.* 18, 1300–1307.
38. Hammond, S., and O'Shea, M. (2007). Escape flight initiation in the fly. *J. Comp. Physiol. A Neuroethol. Sens. Neural Behav. Physiol.* 193, 471–476.
39. de Vries, S.E., and Clandinin, T. (2013). Optogenetic stimulation of escape behavior in *Drosophila melanogaster*. *J. Vis. Exp.* 71, e50192.
40. Kaplan, W.D., and Trout, W.E. (1974). Genetic manipulation of an abnormal jump response in *Drosophila*. *Genetics* 77, 721–739.
41. Anderson, D.J., and Perona, P. (2014). Toward a science of computational ethology. *Neuron* 84, 18–31.
42. Dankert, H., Wang, L., Hoopfer, E.D., Anderson, D.J., and Perona, P. (2009). Automated monitoring and analysis of social behavior in *Drosophila*. *Nat. Methods* 6, 297–303.
43. Kunwar, P.S., Zelikowsky, M., Remedios, R., Cai, H., Yilmaz, M., Meister, M., and Anderson, D.J. (2015). Ventromedial hypothalamic neurons control a defensive emotion state. *eLife* 4, 06633.
44. Wang, L., Chen, I.Z., and Lin, D. (2015). Collateral pathways from the ventromedial hypothalamus mediate defensive behaviors. *Neuron* 85, 1344–1358.
45. Allen, M.J., Godenschwege, T.A., Tanouye, M.A., and Phelan, P. (2006). Making an escape: development and function of the *Drosophila* giant fibre system. *Semin. Cell Dev. Biol.* 17, 31–41.
46. Yilmaz, M., and Meister, M. (2013). Rapid innate defensive responses of mice to looming visual stimuli. *Curr. Biol.* 23, 2011–2015.
47. Card, G., and Dickinson, M. (2008). Performance trade-offs in the flight initiation of *Drosophila*. *J. Exp. Biol.* 211, 341–353.
48. Fink, M., Callol-Massot, C., Chu, A., Ruiz-Lozano, P., Izpisua Belmonte, J.C., Giles, W., Bodmer, R., and Ocorr, K. (2009). A new method for detection and quantification of heartbeat parameters in *Drosophila*, zebrafish, and embryonic mouse hearts. *Biotechniques* 46, 101–113.
49. Blanchard, D.C., Griebel, G., and Blanchard, R.J. (2001). Mouse defensive behaviors: pharmacological and behavioral assays for anxiety and panic. *Neurosci. Biobehav. Rev.* 25, 205–218.
50. Valentinuzzi, V.S., Kolker, D.E., Vitaterna, M.H., Shimomura, K., Whiteley, A., Low-Zeddies, S., Turek, F.W., Ferrari, E.A.M., Paylor, R., and Takahashi, J.S. (1998). Automated measurement of mouse freezing behavior and its use for quantitative trait locus analysis of contextual fear conditioning in (BALB/cJ x C57BL/6J)F2 mice. *Learn. Mem.* 5, 391–403.
51. Zabala, F., Polidoro, P., Robie, A., Branson, K., Perona, P., and Dickinson, M.H. (2012). A simple strategy for detecting moving objects during locomotion revealed by animal-robot interactions. *Curr. Biol.* 22, 1344–1350.
52. Wolf, F.W., Rodan, A.R., Tsai, L.T., and Heberlein, U. (2002). High-resolution analysis of ethanol-induced locomotor stimulation in *Drosophila*. *J. Neurosci.* 22, 11035–11044.
53. Lima, S.L., and Bednekoff, P.A. (1999). Temporal variation in danger drives antipredator behavior: The predation risk allocation hypothesis. *Am. Nat.* 153, 649–659.
54. Houston, A.I., McNamara, J.M., and Hutchinson, J.M.C. (1993). General results concerning the trade-off between gaining energy and avoiding predation. *Philos. Trans. R. Soc. Lond. B. Biol. Sci.* 341, 375–397.
55. Berger, J. (1978). Group-Size, foraging, and antipredator plays: an analysis of bighorn sheep decisions. *Behav. Ecol. Sociobiol.* 4, 91–99.
56. Glück, E. (1987). An experimental study of feeding, vigilance and predator avoidance in a single bird. *Oecologia* 71, 268–272.
57. Gordon, J.A., and Hen, R. (2004). Genetic approaches to the study of anxiety. *Annu. Rev. Neurosci.* 27, 193–222.
58. von Reyn, C.R., Breads, P., Peek, M.Y., Zheng, G.Z., Williamson, W.R., Yee, A.L., Leonardo, A., and Card, G.M. (2014). A spike-timing mechanism for action selection. *Nat. Neurosci.* 17, 962–970.
59. Major, G., and Tank, D. (2004). Persistent neural activity: prevalence and mechanisms. *Curr. Opin. Neurobiol.* 14, 675–684.
60. Lorenz, K.Z. (1950). The comparative method in studying innate behaviour patterns. *Symp. Soc. Exp. Biol.* 4, 221–268.
61. Lorenz, K., and Leyhausen, P. (1973). Motivation of Human and Animal Behavior: An Ethological View, *Volume xix*. (New York: Van Nostrand-Reinhold).
62. Alaux, C., and Robinson, G.E. (2007). Alarm pheromone induces immediate-early gene expression and slow behavioral response in honey bees. *J. Chem. Ecol.* 33, 1346–1350.
63. Goldman, M.S., Compton, A., and Wang, X.-J. (2009). Neural integrator models. In *Encyclopedia of Neuroscience, Volume 6*, L.R. Squire, ed. (Oxford: Academic Press), pp. 165–178.
64. Bargmann, C.I. (2012). Beyond the connectome: how neuromodulators shape neural circuits. *BioEssays* 34, 458–465.
65. Andretic, R., van Swinderen, B., and Greenspan, R.J. (2005). Dopaminergic modulation of arousal in *Drosophila*. *Curr. Biol.* 15, 1165–1175.
66. Inagaki, H.K., Ben-Tabou de-Leon, S., Wong, A.M., Jagadeesh, S., Ishimoto, H., Barnea, G., Kitamoto, T., Axel, R., and Anderson, D.J. (2012). Visualizing neuromodulation in vivo: TANGO-mapping of dopamine signaling reveals appetite control of sugar sensing. *Cell* 148, 583–595.
67. Thran, J., Poeck, B., and Strauss, R. (2013). Serum response factor-mediated gene regulation in a *Drosophila* visual working memory. *Curr. Biol.* 23, 1756–1763.